RSC Advances

ROYAL SOCIETY OF CHEMISTRY

www.rsc.org/advances

Graphical Abstract

With the pre-treatment via photocatalysis, more power of MFCs would be produced and more X-3B would be removed.

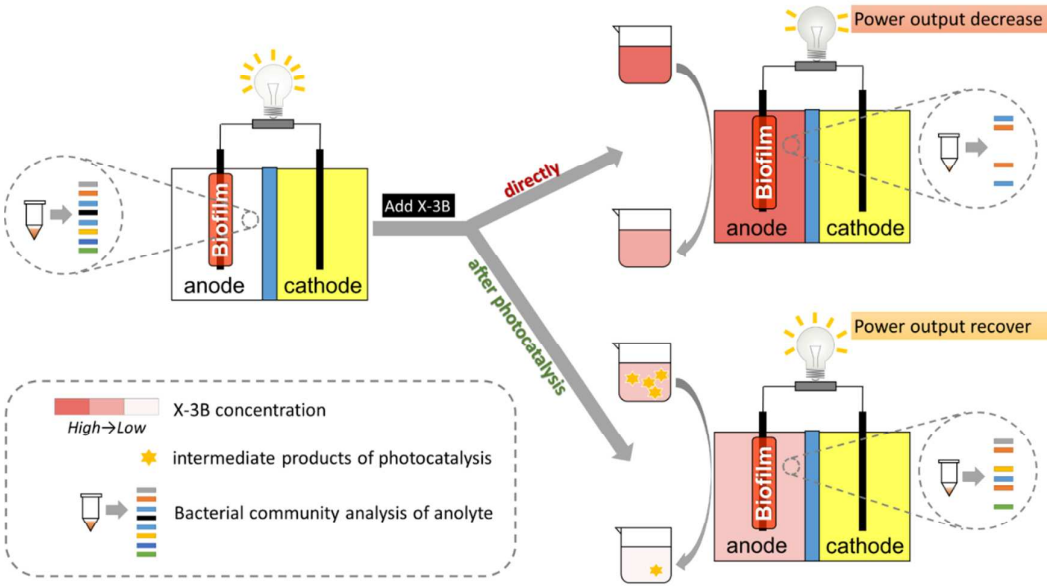

Increasing power density and dye decolorization of X-3B-fed microbial fuel cell via prior TiO_2 photocatalysis

Lin Su[1], Xianpeng Fan[1], Tao Yin[1], Haihua Chen[2], Xiaoxia Lin[1,4], Chunwei Yuan[1], Degang Fu[1, 2, 3 *]

1. State Key Laboratory of Bioelectronics, Southeast University, Nanjing, 210096, China
2. School of Chemistry and Chemical Engineering, Southeast University, Nanjing, 210096, China
3. Suzhou Key Laboratory of Environment and Biosafety, Suzhou, 215123, China
4. School of Material Engineering, Jinling Institute of Technology, Nanjing 211169, China

*Corresponding author. Tel.: +86 025 83793091. E-mail address: fudegang@seu.edu.cn

Abstract: To improve the output power density of dye-fed microbial fuel cells (MFCs) which decreased with increasing dye concentration, a new strategy of prior TiO_2 photocatalysis of high content dye wastewater was proposed and demonstrated in this study. Upon 200 mg/L X-3B wastewater was treated by F doped nano-TiO_2 under visible light for 2.5 h and then mixed into the substrate, the maximum output power density (P_M) of the MFC reached 392 mW/m^2. As a comparison, the P_M was only 276 mW/m^2 when un-treated X-3B wastewater used in the substrate. About 42% power density was retrieved from the MFC fed with high concentration X-3B wastewater via prior photocatalytic treatment. In the meantime, the decolorization rate of X-3B was also enhanced from 42% to 56.5% when combining photocatalysis process. The increase of power density after photocatalysis of X-3B was attributed to less electron consumption by decomposed X-3B, extra electron donors and mediators from produced intermediates as well as increased bacterial diversity in anode chamber. These results demonstrated the prior TiO_2 photocatalysis as effective and easy implementing technology for improving both electricity harvest and pollutant elimination from wastewaters containing concentrated hard-to-use biomass without specially acclimatizing or modifying the MFC.

Keywords: X-3B; MFC; photocatalysis; TiO_2; power recovery

1. Introduction

Microbial fuel cells (MFCs) generate current during the anaerobic metabolism of electricigens which can use a great variety of organics present in wastewaters and removing the discarded pollutants simultaneously [1, 2]. Some chemicals in substrate are poisonous, harmful or biorefractory to the microorganisms, and severely disabled or weakened the performance of MFCs [3, 4]. For example, azo dyes are environmentally hazardous chemicals and widely used in the textile industry, however the treatment of dye containing wastewaters still presents a technical challenge as the dyes are highly stable, as well as resistant to microorganisms [5, 6]. During past decade, MFCs have been utilized for decolorization of dye wastewaters [7,

[8]. It was found that the decolorization of dyes was accelerated in MFCs as compared to traditional anaerobic technology while electricity could be generated simultaneously [9]. But the MFC power density definitely decreased with increasing dye concentration, commonly attributed to the enhanced toxic effect to microbes and more electrons competitively captured by dye molecules [10]. From the point of energy harvest, MFC running under higher dye content will lose much chemical energy in the fuel associated with less electricity generation. Similar problem occurred in MFCs supplied with wastewaters containing biorefractory compounds because extra energy was needed to metabolize these substrates [3, 11, 12].

Recently, researchers have mainly focused on improving MFCs performance to enhance dye decolorization by novel reactor design, anode modification, acclimation of biofilm, coupling with other wastewater treatment technologies etc., while the output power density of the MFCs running with dye wastewaters was still low especially with very high dye content (**Table S1**). More generally speaking, the output power of a MFC fed with easily biodegradable wastewaters could be dramatically reduced due to importing toxic chemicals in the substrate considering the complexity of real wastewaters in practice. Thus, it is desired to promptly restore or increase power density of the MFC without heavily modifying the electrode, system configuration or operating conditions, which is less explored currently [13]. One feasible method was suitable pre-treatment of the wastewater to make the substrates become more appropriate to microorganisms, such as dilution [14], autoclave [15], and sonicate [16]. For example, Mahmoud tested fermentation as the pretreatment technology for recalcitrant substrates to enrich the carbohydrates that are easier for biodegradation [17]. However simply avoiding such situation by separating toxic chemicals out from substrates like adsorption will lose the chemical energy stored in these compounds, possible problem of so-called secondary pollution aside.

Photocatalysis based on nano-TiO_2 is a powerful technique that could decompose almost all organic chemicals and has been extensively studied in cleaning air and water [18]. Especially, modified TiO_2 with visible light catalysis activity by element doping (such as fluorine, nitrogen) or narrow band semiconductors can utilize solar energy for pollutant treatment [19, 20], enabling energy-saving photocatalysis. By this technology, it's possible to disintegrate the toxic or biorefractory chemicals into non-toxic and bioavailable substrates. For example, Vinodgopal reported the TiO_2 photocatalytic degradation of an azo dye Acid Orange 7, 1, 2-naphthoquinone and phthalic acid have been identified as the intermediates [21]. The toxicity of sulfonamides was significantly lowered after TiO_2 photocatalysis [22], which could be further used in biological procedures. In our previous researches [23, 24], progressive

decoloration of azo dyes under visible light was easily achieved using the magnetically separable composite photocatalyst. However, researches on TiO_2 photocatalysis concentrated on how to decompose the organics thoroughly (**Table S1**), and there is no consideration of using TiO_2 photocatalysis as a pre-treatment technology to increase the power density of a MFC fed with dye wastewater until now. It is not clear whether and how the output of a MFC could be significantly improved when the toxic or biorefractory substrates are incompletely decomposed on purpose by TiO_2 photocatalysis instead of thoroughly degraded into carbon dioxide, ahead of feeding into MFC.

Here in this work, we demonstrated for the first time, to the best of our knowledge, the strategy shown in **Fig.1** that utilize prior photocatalysis of X-3B (Reactive Brilliant Red dye) to improve electricity production in MFC supplied with high content dye wastewater without specially acclimatizing or optimizing the cell operation, while enhancing the dye decolorization simultaneously. X-3B was chosen because it is one of the most widely used azo dyes in textile industry, but with the toxicity to organisms and degradation resistance in the nature [25, 26]. The influence of un-treated X-3B and pre-treated X-3B on power output of the MFC was evaluated. The power recovery owing to visible light photocatalysis of X-3B prior to its use as fuel was investigated, and the potential benefits of the method were also discussed.

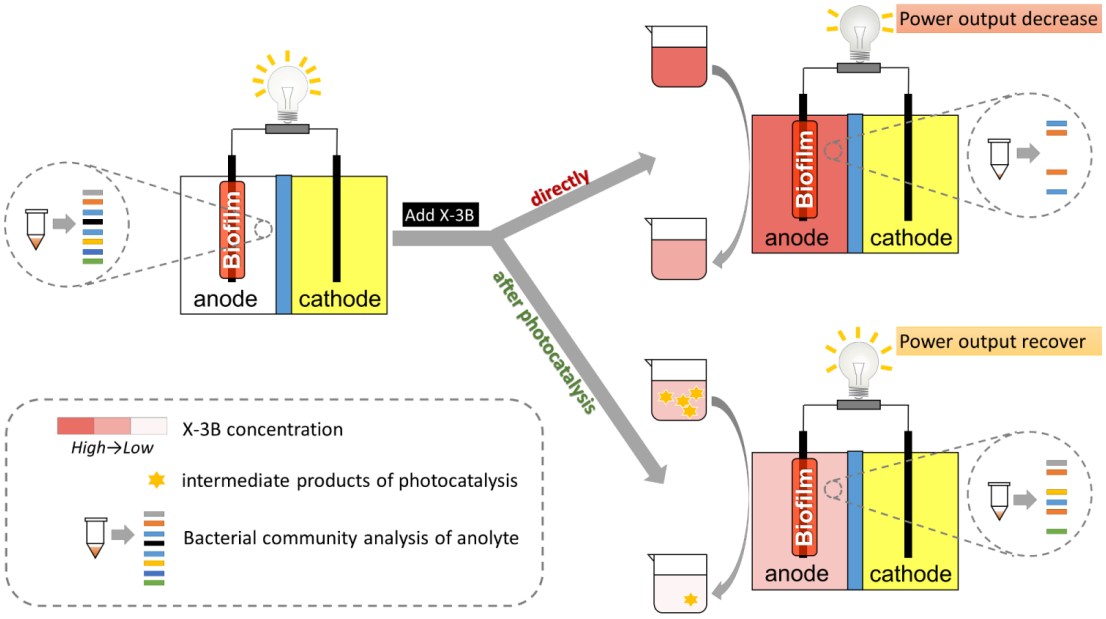

Fig.1 Schematic view of two pathways for utilizing X-3B in MFC, i.e., without treatment and pre-treatment via TiO_2 photocatalysis before X-3B was added into anode chamber. It was expected that more power would be produced and more X-3B would be removed with prior photocatalysis.

2. Materials and methods

2.1 MFC set-up, operation and characterization

An "H" type MFC with two chambers was used, the volume of each chamber separated by a proton exchange membrane (Nafion117, DuPont) was 245 mL. Both anode and cathode were made from carbon paper (HCP020N, Hesen, Shanghai) with the size of 4.0 cm×4.0 cm; and the distance between electrodes was set at 4 cm. A copper wire was used to connect external circuit containing a resistance of 1500 Ω. The nonconductive epoxy resin was utilized for isolating exposed metal surfaces from solutions.

The sludge inoculum was obtained from the Wastewater Treatment Plant of Nanjing City and under anaerobic culture for more than 24 hours. A mixture of cultured sludge and medium solution (1:4, V/V) was used as the initial anodic inoculum. The medium solutions with pH=7.0 contained (per liter of deionized water): NH_4Cl (0.31 g), KCl (0.13 g), Na_2HPO_4 (11.54 g), and NaH_2PO_4 (2.78 g). Catholyte contained the same medium solution as well as 50 mmol/L potassium ferricyanide. The experimental temperature was controlled at 30℃. During start-up stage, only glucose (1.0 g/L) was added as carbon sources for the growth of anode-associated biofilm. When the cell voltage was lower than 50 mV, fresh substrates were added into anode chamber and the cell operated in a new running cycle. The output voltage was stable and maintained for 2-3 months after about more than 10 cycles, start-up was then finished and the MFC was ready for subsequent experiments.

Voltages across the resistance in external circuit were automatically recorded by a data acquisition system (U120816, HYTEK Automation). The output power density (mW/m^2) was calculated as $P=1000U^2/(RA)$, where A is the projected surface area of the anode (m^2); U is the voltage (V); R is the resistance (Ω) used in external circuit. The power density curve of the MFC was measured by replacement of external resistance [27]. The effects of three kinds of substrates were evaluated. **Glu-X_M-0** was pure glucose (400 mg/L) used as the blank control. **Glu-X_{PM}-200** was a mixture of TiO_2 pre-treated X-3B (200 mg/L) with glucose (400 mg/L), which was used to analyze the ability of photocatalysis to power recovery, and **Glu-X_M-Y** was the mixture of glucose (400 mg/L) with un-treated X-3B (**Y** mg/L) for purpose of comparison. Before renewal of the substrate for a new run, the MFC was cultivated with medium containing 1.0 g/L glucose to ensure the cell to display the original state if necessary.

The electrochemical experiments were conducted by CHI760D systems (Shanghai CH

Instrument Co., Ltd) using three electrodes system with anode as the working electrode and cathode as the counter electrode. All the potentials were recorded against saturated calomel electrode (**SCE)**. Cyclic voltammogram (CV) was measured at scan rate of 10mVs^{-1}.

2.2 Photocatalytic pretreatment of X-3B

The fluorine (F) doped nano-TiO_2 composite with magnetic active carbon granule (ACG), i.e., F-TiO_2/magnetite/ACG, was synthesized according to our previous research (see supporting materials). The photocatalytic system used in the experiment consists of a glass beaker (1000 mL capacity) covered by aluminized paper, and a light source (MVL-210, 290 W, MEJIRO GENOSSEN) at upper surface of the reactor. The photocatalytic degradation experiment was performed with the following procedure: composite catalyst powder (final concentration was 1.5 g/L) was mixed with X-3B dye (200 mg/L) in the dark for 30 min to reach adsorption–desorption equilibrium, then the reactor was irradiated with visible light under continuous stirring. During the photocatalysis, samples were collected at a time interval of every 30 min. A UV–visible spectrophotometer (Shimadzu Corporation) was used for absorbance measurements of X-3B at the wavelength of 535.5 nm [24] and a LC-MS (1260-6224, Agilent Technologies) instrument was used to analyze the products in solution after degradation.

2.3 Bacterial community and phylogenetic analysis

In company with MFC evaluation, the samples containing different substrates, i.e., **Glu-X_{PM}-200**, **Glu-X_M-200** and **Glu-X_M-0**, were taken from anode chamber of the MFC at middle point of a running cycle for DGGE (denaturing gradient gel electrophoresis) analysis, using a DCode universal mutation detection system (Bio-Rad Laboratories, United States). The biofilm sample that carefully scraped from the anode surface of the MFC was also applied DGGE analysis. DNA was extracted using the FastDNA extraction kit (2 mL spin, MP Bio medicals) and stored at −20°C until further analysis.

Extracted DNA was amplified via PCR with an annealing temperature of 56.5℃ to obtain fragments with lengths around 200 base pairs. Bacterial primers used were F341 (5'-CCTAC GGGAG GCAGC AG-3') and R518 (5'-ATTAC CGCGG CTGCT GG-3') [28, 29]. Additional G-C clip (5'-CGCCC GCCGC GCGCG GCGGG CGGGG CGGGG GCCCG GGGGC-3') was added before F341 to enhance the DGGE resolution. All samples were stored at 4℃ until use. The denatured gradient in the DGGE gel ranged from 30% to 60%, where 100% denaturation corresponds to 40% (v/v) formamide and 7 M urea. Target gel bands were extracted and purified using the Poly-Gel DNA Extraction

Kit (Omega), then sent for cloning and sequencing (BGI, China). Sequencing results were uploaded to the EMBL (European Molecular Biology Laboratory) Nucleotide Sequence Database with the accession No. from LM655401 to LM655406.

3. Results and discussion

3.1 The effect of glucose on performance of MFC

Glucose is commonly used as co-substrate for bio-decolorization of azo dye [10, 30]. After the MFC was successfully started, the voltage output of the MFC as the function of glucose content was examined. As shown in **Fig.2**, when substrate containing 100 mg/L X-3B and different amount of glucose varied from 1g/L to 0.2g/L, the output voltage for each substrate replacing-running cycle was near constant while the time period of a cycle decreased with reduced glucose concentration. Upon same load was linked in external circuit, the similar voltage output regardless of varied glucose concentration meant that the electrochemically active biofilm on anode of the MFC has been well developed. The diverse microorganisms enriched during the start-up of the MFC ensure the biofilm being of solid stability as observed from other sludge inoculated microbial consortia [31]. The voltage dropped at the end of each cycle when all glucose has been expended, but the output could be quickly restored once the fresh substrate was supplied.

In the MFC, glucose was sole carbon source in anode chamber, so that the activity of the microbes including electricigens would be sharply declined as long as the glucose had been used up. Less glucose, much faster it was depleted, then shorter duration of the current production (**Fig.2**). Opposite to running period, the coulombic efficiency was decreased with increasing glucose concentration (**Fig.S1**). In this research, we set glucose concentration in substrate as 400 mg/L for subsequent assessment experiments. It should be noted that only X-3B without glucose in the substrate couldn't support the operation of the MFC (indicated as the circle in **Fig.2**). However, the output of the MFC could be rapidly restored after re-addition of 1.0g/L glucose, which further confirmed that the adapted anodophilic consortia was enough stable to suffer from the variation of the substrate.

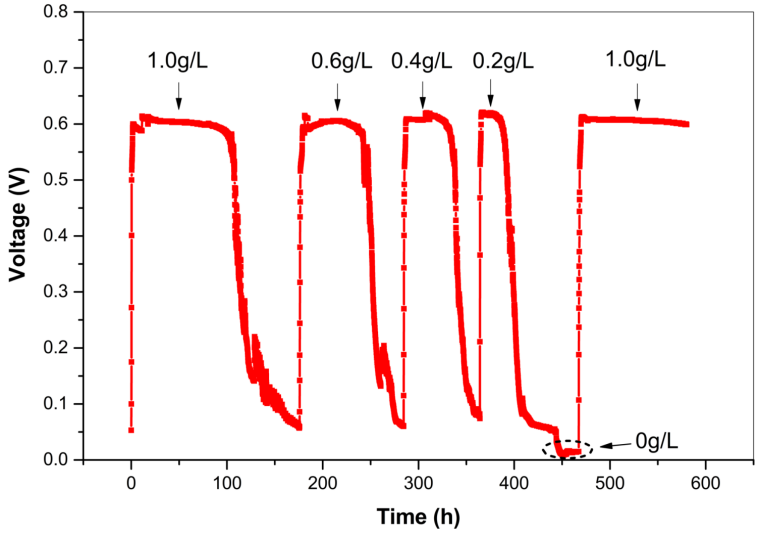

Fig.2 Output voltage - time curve of the MFC using different content of glucose mixing with 100 mg/L X-3B as substrate. The concentration of glucose in each running cycle was indicated. The external load of the MFC was 1500Ω.

3.2 Influence of X-3B concentration on MFC performance

Once glucose concentration fixed at 400 mg/L in substrate, the substrates **Glu-X_M-Y** was used to explore the influence of X-3B on MFC performance, where Y represented the X-3B concentration in mg/L in substrate. Specially, **Glu-X_M-0** was the pure glucose substrate without X-3B and used as the blank control. **Fig.3a** showed that voltage at each cycle was maintained around 650 mV despite of the concentration of X-3B. This indicated that the biofilm on anode still kept stable and presented a higher tolerance to gradually increasing of X-3B [32]. However, the running period was obviously decreased once 50 mg/L X-3B added into substrate, while open circuit voltage (OCV) and maximum power density were also reduced (**Fig.3b**). The facts undoubtedly revealed the negative effect of X-3B on electricity generation in accordance with previous reports [8, 33, 34]. The accompanied decrease of OCV with addition of X-3B implied much energy was consumed in intracellular metabolism [11]. As X-3B reached higher concentration, considerable deterioration on power output has happened as seen from **Fig.3b**. The maximum power density of the MFC in the blank control experiment using substrate **Glu-X_M-0** was 502 mW/m^2. It was 450 and 433 mW/m^2 using substrates **Glu-X_M-50** and **Glu-X_M-100** respectively, with 10.3% or 13.7% power density lost relative to the blank control. However, using the substrate **Glu-X_M-200**, the maximum power density dropped to 276 mW/m^2 was only 55% that of the blank control, corresponding to 45% loss of the power density. The current density of the MFC fed with **Glu-X_M-200** began drop quickly on reaching about 0.5 A/cm^2, due to significant increase in mass transfer resistance at higher current density in this case. Although the rate of decrease in duration reduced as X-3B

concentration increased from 50 mg/L to 100 mg/L and then 200 mg/L, reflecting the adaptive capacity of the biofilm to environmental stress, the maximum power density and current density all dramatically decreased when X-3B concentration was 200 mg/L. To utilize the biomass energy more efficiently, pre-treating 200 mg/L X-3B by TiO_2 photocatalysis to fragment X-3B was considered for purpose of power recovery, instead of diluting X-3B solution. It is expected that after fragmented by TiO_2 photocatalysis, these substrates could not only be more easily utilized by microorganisms, but also retain the available chemical energy in organic fuel as much as possible.

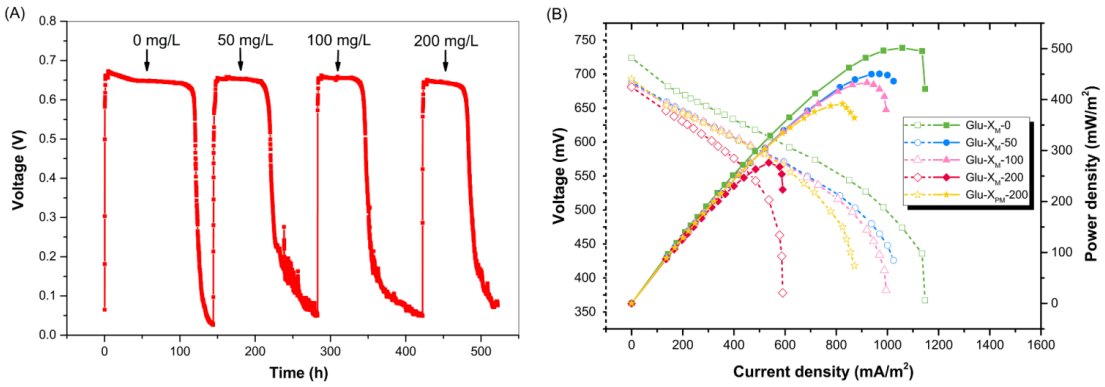

Fig.3 (A) Output voltage - time curve of the MFC supplied with different substrates in each cycle. The substrate consisted of 400 mg/L glucose and un-treated X-3B with the concentration was indicated in each running. (B) Power density curves and polarization curves of the MFC operated under different substrates. **Glu-X_M-Y** represented the substrate containing 400 mg/L glucose and Y mg/L X-3B. Specially, **Glu-X_M-0** indicated the blank control containing only 400 mg/L glucose without X-3B in substrate. **Glu-X_{PM}-200** was the substrate containing 400 mg/L glucose and 200 mg/L pre-treated X-3B by TiO_2 photocatalysis. The power density of the MFC supplied with **Glu-X_M-200** was severely reduced relative to the blank control, while it was obviously recovered when supplied with **Glu-X_{PM}-200**.

3.3 Power recovery by photocatalysis pretreatment

The 200mg/L X-3B solution was treated under visible light for 2.5h by as prepared photocatalyst. Then the catalyst was separated and the solution was mixed with glucose as the substrate (**Glu-X_{PM}-200**) for operation of the MFC. The voltage and the duration of the MFC using **Glu-X_{PM}-200** were similar to those using **Glu-X_M-200** (**Fig.S2**), as well as using **Glu-X_M-100** (**Fig.3a**). But obvious current increase could be found from cyclic voltammogram of anode biofilm in **Glu-X_{PM}-200** (**Fig.4**). The CV exhibited anodic catalytic wave with typical sigmoidal shape normally found in electrochemistry of electricity-generating biofilms. While the cathodic peak current has a little increase, the absolute anodic peak current changed from 3.27 mA in

Glu-X_M-200 to 4.21 mA in **Glu-X_{PM}-200** with about 28.7% increase. The higher anodic current means more electrons could transfer to external circuit from substrate **Glu-X_{PM}-200** and thus one can expect higher power output of the MFC. The oxidation and reduction potentials of the anode biofilm in **Glu-X_{PM}-200** (-0.333V, -0.541V) and in **Glu-X_M-200** (-0.325V, -0.546V) were almost the same and are close to the CV peak positions of electricigens reported in literatures [35, 36], suggested the EET pathways of anode biofilm in two substrates (**Glu-X_{PM}-200** and **Glu-X_M-200**) were almost unchanged [37].

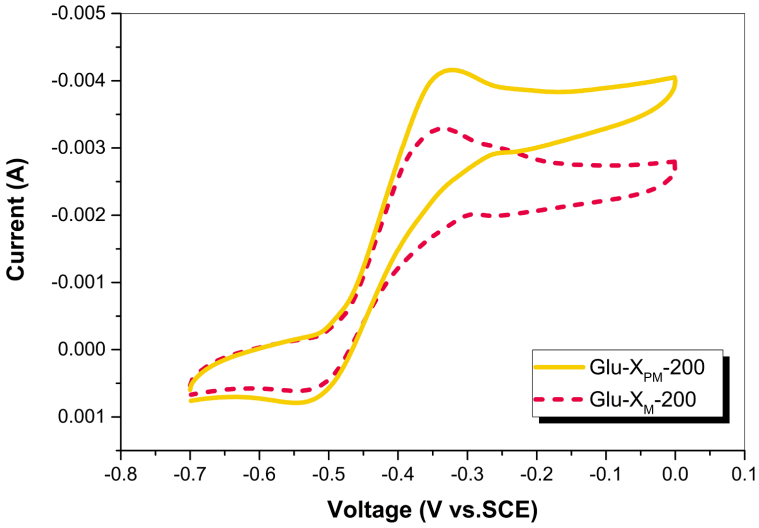

Fig.4 CV spectra of the anode biofilm in different substrates. The anodic peak current was increased in **Glu-X_{PM}-200** while the peak position was nearly the same in two cases.

In accord with CV observation, the maximum power density of the MFC using substrate **Glu-X_{PM}-200** was 392mW/m^2, being equal to about 78.1% that of the blank control as shown in **Fig.3b**. Compared with using **Glu-X_M-200**, about 23% power density of the control was restored and 42% power density was increased when X-3B was treated by TiO_2 photocatalysis ahead of its addition into MFC. With same strategy, much more power density (about 64.4%) could be recovered in a single strain inoculated MFC (**Fig.S3**) further demonstrating the effectivity of the method. With respect to power recovery, the photocatalytic pretreatment to decompose X-3B into fragments could bring some bonuses that contribute the enhancement of MFC performance. First, fewer electrons were used to reduce the azo linkages as the concentration of X-3B decreased by photocatalysis. In contrast, X-3B in **Glu-X_M-200** consumed more electrons released from glucose by bacteria metabolism and fewer electrons were used for current output. Second, after photocatalytic pretreatment of X-3B, the concentration of possible toxic chemicals in substrate was decreased which induced less environmental stress to microbial communities in anolyte. As a result,

more microorganisms could survive in anode chamber, especially those microbes sensitive to X-3B. Third, photocatalysis produced some intermediate compounds that became usable directly for bacterial consortia (**Fig.S4** and **Fig.5**) served as supplementary electron donors like aliphatic acids [38, 39], or perhaps as mediators similar to quinones facilitating electron transfer from bacteria to the anode [40, 41]. Due to above positive effects caused by photocatalytic pretreatment, the bioavailability of X-3B containing substrate was increased and therefore, power output of the MFC using **Glu-X_{PM}-200** was improved.

3.4 The degradation of X-3B

According to previous researches, the degradation of X-3B during TiO_2 photocatalysis concerned the formation of intermediates such as aniline-like, naphthalene-like as well as triazene-like compounds (**Fig.S4**). The naphthalene ring could transform to benzene-like compounds as well as other benzoic acid derivatives, and aniline-like compounds could be oxidized as phenol and quinones, etc., while benzoic acid derivatives could further turn into aliphatic acids. Some released byproducts such as aliphatic acids (C, D) and polyphenol (E) in X-3B solution after 2.5h photocatalytic pretreatment could be identified from LS-MS shown in **Fig.5a**. The result followed general degradation mechanism of X-3B and validated our inference that deliberate photocatalysis could disintegrate X-3B into fragments as extra electron donors available to microbes. The concentration of X-3B was decreased from 200 mg/L at the beginning to 120 mg/L, corresponding to 40% degradation of total X-3B in photocatalytic process (**Fig.5b**). X-3B was further decomposed in **Glu-X_{PM}-200** during MFC running, and lowered to about 91 mg/L after 70 h operation or 87 mg/L after a whole running, i.e., 82 h, which means 24% or 27.5% additional degradation in MFC. The overall degradation efficiency of X-3B in **Glu-X_{PM}-200** was 54.5% or 56.5% upon combining 2.5h photocatalysis and 70h or 82h MFC handling. As a comparison, the final concentration in **Glu-X_{M}-200** after a whole MFC operation, i.e., 76 h running was 116 mg/L, corresponding to total 42% degradation (**Fig.5b**). Therefore, the percent degradation of X-3B in **Glu-X_{PM}-200** was higher than in **Glu-X_{M}-200**. The result further demonstrated the advantage of photocatalytic pre-treatment of X-3B: it was not only helpful for electricity generation, but also beneficial to the degradation of the dye.

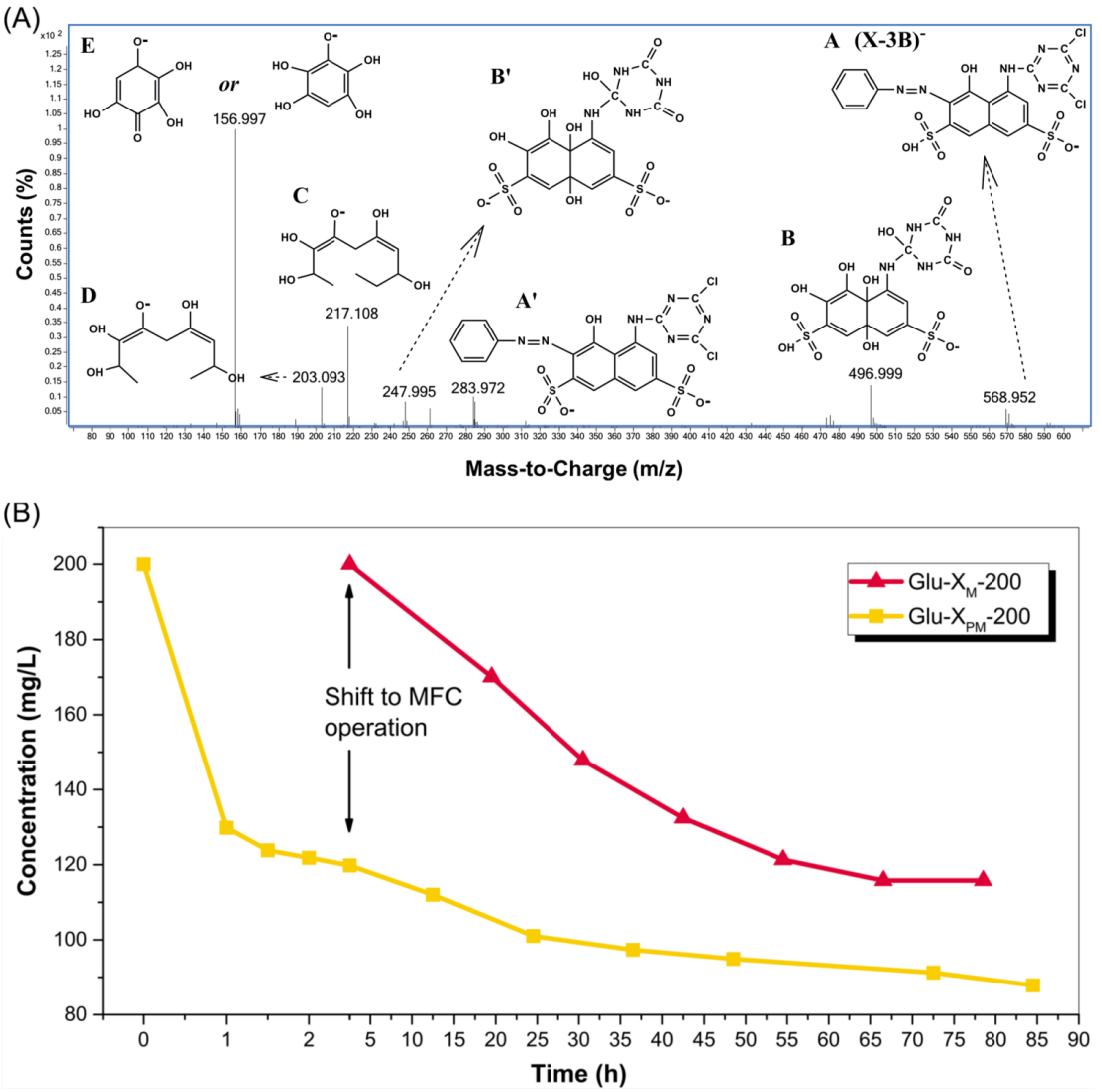

Fig.5 (A) ESI-Mass spectrum in negative ion mode of degraded X-3B solution after TiO_2 photocatalysis under visible light for 2.5h. The possible structures corresponding to main ion peaks were also shown. (B) The degradation curves of X-3B in two experiments indicated the X-3B remained in substrates with time. The X-3B was first treated by TiO_2 photocatalysis under visible light for 2.5h and then further degraded in **Glu-X_{PM}-200** during the operation of MFC, while X-3B in **Glu-X_M-200** was just decomposed in MFC.

On considering the degradation of X-3B in MFC, the percent degradation was higher in **Glu-X_M-200** than in **Glu-X_{PM}-200**. This was consistent with the suggestion that less released electrons were consumed by X-3B in **Glu-X_{PM}-200**. Another observation in **Fig.5b** was that the degradation curve of **Glu-X_M-200** reaches plateau at the end stage of MFC operation due to exhaustion of glucose, but there was still a slow X-3B degradation in **Glu-X_{PM}-200** even at the end of operation. It reflects in some way the fact that besides glucose, some intermediate compounds (**Fig.5a**) produced during photocatalytic process could be the carbon source in **Glu-X_{PM}-200** to provide

additional electrons and support the degradation of X-3B in MFC.

3.5 Community analysis

Analysis using DGGE was able to profile the diversity of microbial community. The different cDNA fragments shown as separate bands in DGGE gel-image visually exhibited the diversity of bacterial consortia (**Fig.6a**). The anode-associated biofilm of the MFC contained most abundant microbial species as expected. According to previous studies, rich and diverse source of bacteria is helpful to produce high power densities [42, 43] owing to syntrophic microbial interactions and/or synergistic bacterial communication. For example, mediators produced by one germ in biofilm or in anolyte could be used by other species as electron shuttles [44]. The biofilm maintaining a high biodiversity supported its outstanding stability as aforementioned. While the microbial populations in anolytes with different X-3B content were assessed and compared as in **Fig.6a**, a significant and successive decrease of the microbial species was clearly observed in **Glu-X_M-0**, **Glu-X_{PM}-200** and **Glu-X_M-200**. There was less diversity of microbial communities in **Glu-X_{PM}-200** and **Glu-X_M-200** than in **Glu-X_M-0** reflected the toxicity of azo dye. However, after photocatalytic pretreatment of X-3B, more microbes (band 7, 11, 12) were survived in **Glu-X_{PM}-200** than in **Glu-X_M-200**. The result of electrophoretogram was in line with observed MFC output discussed above.

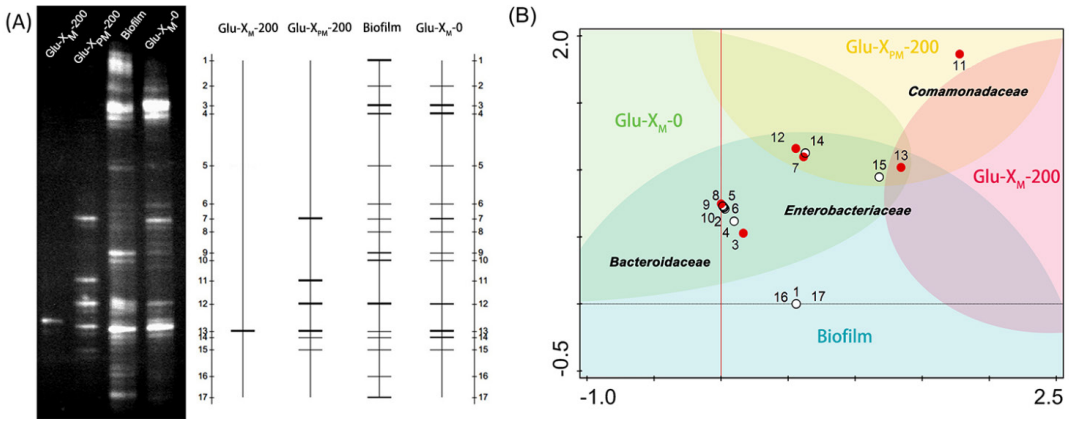

Fig.6 (A) DGGE gel-image showed the difference of microbial community in each sample. With the biofilm contained most abundant microbial species, more strains were survived in anolyte containing less X-3B. The X-3B in **Glu-X_{PM}-200** was first treated by TiO_2 photocatalysis prior to its use in MFC. (B) The DCA analysis (Canoco 5.0, discrete choice approach) showed the distribution of microbial species in different samples.

To understand the role of microorganisms in anolyte, the main bands in the DGGE gels (band 3, 7, 9, 11, 12 and 13) were excised, sequenced, and then the phylogenetic analysis was performed based on 16S clone library (**Fig.S5**), which

indicated that most of them belonged to *Enterobacteriaceae* (band 7, 12, and 13), *Bacteroidaceae* (band 3 and 9) and *Comamonadaceae* (band 11). More detailed detrended correspondence analysis (DCA) combining sequencing results with the bands information was shown in **Fig.6b**. Biofilm included almost all species except *Comamonadaceae* (band 11), which was only enriched in **Glu-X_{PM}-200**. It was known that the strain has the tolerance ability to benzene compounds (photocatalysis products of X-3B) [45]. So after photocatalytic treatment of X-3B, the bacteria became much easily appeared and abundant in **Glu-X_{PM}-200**, and may play a role in the degradation of aromatic compounds. On the contrary, in **Glu-X_{M}-200**, X-3B killed almost all the bacteria but one strain (band 13) belongs to *Enterobacteriaceae*, which is usually found in environment containing azo dyes[46]. However, all *Enterobacteriaceae* species (band 7, 12, and 13) were found in the anolyte containing **Glu-X_{M}-0** or **Glu-X_{PM}-200**, as well as in biofilm. Much rich *Enterobacteriaceae* species explained the stability and tolerance of the biofilm to X-3B as well as notable power recovery of MFC using **Glu-X_{PM}-200** relative to using **Glu-X_{M}-200**, and again demonstrating the role of pre-treatment of X-3B. The bacteria from *Bacteroidaceae* (band 3, band 9, etc.) shown in the down left region were found in biofilm and in anolyte containing only pure glucose (**Glu-X_{M}-0**). Previous studies [47, 48] have proved that some of the *Bacteroidaceae* bacteria were the members of electricigens, so these species may be responsible for the current generation. It was noted that these species were not seen in anolyte containing **Glu-X_{PM}-200** or **Glu-X_{M}-200**, which means that they are very sensitive to X-3B.

Conclusions

As a promising technology, MFCs is highly desired to produce electricity as much as possible and simultaneously remove various discarded pollutants such as high concentration dye in wastewaters very effectively. As a demonstration, we showed that 200 mg/L X-3B in substrate dramatically reduced the power density (about 45% of the control) and current density of the MFC, but the power density was significantly restored (23% of the control) when X-3B was pre-treated by TiO_2 photocatalysis under visible light for 2.5h, with synchronous enhancement of X-3B elimination. It was found that the decrease of consumed electrons by X-3B, the increase of strains survived in anode chamber, and extra electron donors from degradation intermediates by photocatalysis were beneficial to the performance recovery of the MFC. It should be mentioned that the MFC used in this research was not specially acclimatized to X-3B. In principal, the strategy used in this research should be applicable to wastewaters containing other types of biorefractory

compounds with higher concentration.

The real wastewaters are very complex, may contain poisonous, recalcitrant compounds with changeful content. The result in this research demonstrated the potent ability of TiO_2 photocatalysis on decomposing hard-to-use biomass into bioavailable fragments, while keeping transformable chemical energy in these substrates as soon as possible for energy harvest. Compared to the fermentation process, the technique is applicable to almost all substrates while the former doesn't work well with the toxic compounds or indigestible organics. It should be noted that this photocatalytic pre-treatment of high content dye wastewater is feasible in practice (**Fig.5b** and **Fig. S7**), as the chemical not need to degrade totally which is difficult at present for TiO_2 photocatalysis (**Table S1**). While incompletely degradation, the as prepared magnetic separable photocatalyst can be easily isolated from product (**Fig. S6**), which is convenient to arrange the pre-treatment process with MFC operation. More importantly, not only the lost energy could be recovered from a MFC un-optimized to harmful substrates by performing so designed photocatalysis prior to feeding the substrate, but also such pre-treatment process could be easily implemented using solar energy in an energy-saving manner (**Fig. S7**). These advantages confer the technology as a green and cost-effective pretreatment approach to retrieve electric energy from poisonous or indigestible wastewaters by MFC as much as possible.

ACKNOWLEDGMENTS

This work was supported by National Natural Science Foundation of China (No. 51172043), and the State Key Laboratory of Bioelectronics, Southeast University.

References:

1. W. Li, H. Yu and Z. He, *Energy Environ. Sci.*, 2014, **7**, 911-924.
2. D. Pant, G. Van Bogaert, L. Diels and K. Vanbroekhoven, *BIORESOURCE TECHNOL*, 2010, **101**, 1533-1543.
3. Y. Luo, R. Zhang, G. Liu, J. Li, M. Li and C. Zhang, *J HAZARD MATER*, 2010, **176**, 759-764.
4. T. Catal, Y. Fan, K. Li, H. Bermek and H. Liu, *J POWER SOURCES*, 2008, **180**, 162-166.
5. M. A. Brown and S. C. De Vito, *CRIT REV ENV SCI TEC*, 1993, **23**, 249-324.
6. C. Wang, A. Yediler, D. Lienert, Z. Wang and A. Kettrup, *CHEMOSPHERE*, 2002, **46**, 339-344.
7. S. Kalathil, J. Lee and M. H. Cho, *BIORESOURCE TECHNOL*, 2012.
8. K. Solanki, S. Subramanian and S. Basu, *BIORESOURCE TECHNOL*, 2013, **131**, 564-571.
9. B. Chen, M. Zhang, C. Chang, Y. Ding, K. Lin, C. Chiou, C. Hsueh and H. Xu, *BIORESOURCE TECHNOL*, 2010, **101**, 4737-4741.
10. J. Sun, Y. Hu, Z. Bi and Y. Cao, *BIORESOURCE TECHNOL*, 2009, **100**, 3185-3192.
11. U. Schröder, *PHYS CHEM CHEM PHYS*, 2007, **9**, 2619-2629.
12. J. Yu, J. Seon, Y. Park, S. Cho and T. Lee, *BIORESOURCE TECHNOL*, 2012, **117**, 172-179.
13. H. Cheng, B. Liang, Y. Mu, M. Cui, K. Li, W. Wu and A. Wang, *WATER RES*, 2015, **81**, 72-83.
14. B. Min, J. Kim, S. Oh, J. M. Regan and B. E. Logan, *WATER RES*, 2005, **39**, 4961-4968.
15. S. Oh, J. Y. Yoon, A. Gurung and D. Kim, *BIORESOURCE TECHNOL*, 2014, **165**, 21-26.
16. T. T. More and M. M. Ghangrekar, *BIORESOURCE TECHNOL*, 2010, **101**, 562-567.
17. M. Mahmoud, P. Parameswaran, C. I. Torres and B. E. Rittmann, *BIORESOURCE TECHNOL*, 2014, **151**, 151-158.
18. K. Hashimoto, H. Irie and A. Fujishima, *JPN J APPL PHYS*, 2005, **44**, 8269.
19. S. H. S. Chan, T. Yeong Wu, J. C. Juan and C. Y. Teh, *J. Chem. Technol. Biotechnol.*, 2011, **86**, 1130-1158.
20. D. Robert and S. Malato, *SCI TOTAL ENVIRON*, 2002, **291**, 85-97.
21. K. Vinodgopal, D. E. Wynkoop and P. V. Kamat, *ENVIRON SCI TECHNOL*, 1996, **30**, 1660.
22. W. Baran, J. Sochacka and W. Wardas, *CHEMOSPHERE*, 2006, **65**, 1295-1299.
23. Y. Ao, J. Xu, D. Fu and C. Yuan, *J ALLOY COMPD*, 2009, **471**, 33-38.
24. J. Xu, Y. Ao, D. Fu and C. Yuan, *APPL SURF SCI*, 2008, **254**, 3033-3038.
25. Y. Cheng and Q. Zhou, *Journal of Environmental Sciences*, 2002, **14**, 136-140.
26. J. W. Daly, D. M. Jerina and B. Witkop, *Experientia*, 1972, **28**, 1129-1149.
27. F. Zhao, R. C. T. Slade and J. R. Varcoe, *CHEM SOC REV*, 2009, **38**, 1926.
28. M. D. Yates, P. D. Kiely, D. F. Call, H. Rismani-Yazdi, K. Bibby, J. Peccia, J. M. Regan and B. E. Logan, *The ISME Journal*, 2012, **6**, 2002-2013.
29. N. T. Phung, J. Lee, K. H. Kang, I. S. Chang, G. M. Gadd and B. H. Kim, *FEMS MICROBIOL LETT*, 2004, **233**, 77-82.
30. J. Sun, Y. Li, Y. Hu, B. Hou, Y. Zhang and S. Li, *APPL MICROBIOL BIOT*, 2013, **97**, 3711-3719.
31. J. R. Kim, B. Min and B. E. Logan, *APPL MICROBIOL BIOT*, 2005, **68**, 23-30.
32. S. Ishii, S. Suzuki, T. M. Norden-Krichmar, K. H. Nealson, Y. Sekiguchi, Y. A. Gorby and O. Bretschger, *PLOS ONE*, 2012, **7**, e30495.
33. A. Pandey, P. Singh and L. Iyengar, *INT BIODETER BIODEGR*, 2007, **59**, 73-84.
34. A. B. Dos Santos, F. J. Cervantes and J. B. van Lier, *BIORESOURCE TECHNOL*, 2007, **98**, 2369-2385.
35. H. Richter, K. P. Nevin, H. Jia, D. A. Lowy, D. R. Lovley and L. M. Tender, *ENERG ENVIRON SCI*,

2009, **2**, 506.

36. S. Srikanth, E. Marsili, M. C. Flickinger and D. R. Bond, *BIOTECHNOL BIOENG*, 2008, **99**, 1065-1073.

37. A. A. Carmona-Martinez, F. Harnisch, L. A. Fitzgerald, J. C. Biffinger, B. R. Ringeisen and U. Schröder, *BIOELECTROCHEMISTRY*, 2011, **81**, 74-80.

38. Z. He, N. Wagner, S. D. Minteer and L. T. Angenent, *ENVIRON SCI TECHNOL*, 2006, **40**, 5212-5217.

39. H. Luo, G. Liu, R. Zhang and S. Jin, *CHEM ENG J*, 2009, **147**, 259-264.

40. F. P. Van der Zee and F. J. Cervantes, *BIOTECHNOL ADV*, 2009, **27**, 256-277.

41. K. Watanabe, M. Manefield, M. Lee and A. Kouzuma, *CURR OPIN BIOTECH*, 2009, **20**, 633-641.

42. B. E. Logan, *NAT REV MICROBIOL*, 2009, **7**, 375-381.

43. K. Rabaey and W. Verstraete, *TRENDS BIOTECHNOL*, 2005, **23**, 291-298.

44. D. R. Bond and D. R. Lovley, *APPL ENVIRON MICROB*, 2003, **69**, 1548-1555.

45. S. A. B. Weelink, N. C. G. Tan, H. Ten Broeke, C. van den Kieboom, W. van Doesburg, A. A. M. Langenhoff, J. Gerritse, H. Junca and A. J. M. Stams, *APPL ENVIRON MICROB*, 2008, **74**, 6672-6681.

46. Y. Su, Y. Zhang, J. Wang, J. Zhou, X. Lu and H. Lu, *BIORESOURCE TECHNOL*, 2009, **100**, 2982-2987.

47. Y. Zhang, B. Min, L. Huang and I. Angelidaki, *BIORESOURCE TECHNOL*, 2011, **102**, 1166-1173.

48. H. Rismani-Yazdi, S. M. Carver, A. D. Christy, Z. Yu, K. Bibby, J. Peccia and O. H. Tuovinen, *BIORESOURCE TECHNOL*, 2013, **129**, 281-288.